JOURNAL OF SPACECRAFT AND ROCKETS
Vol. 33, No. 6, November–December 1996

Liquid Crystal Thermography for Heat Transfer Measurement in Hypersonic Flows: A Review

G. T. Roberts and R. A. East
University of Southampton, Southampton, Hampshire SO17 1BJ, England, United Kingdom

Nomenclature

c = substrate specific heat capacity, $Jkg^{-1}K^{-1}$
D = fin leading-edge diameter, 10 mm
H = hue; Eq. (7)
h = heat transfer coefficient, $Wm^{-2}K^{-1}$
I = intensity; Eq. (10)
k = substrate thermal conductivity, $Wm^{-1}K^{-1}$
n = mean refractive index of liquid crystal
P = pitch of helical structure, m
q_w = convective heat flux, Wm^{-2}
R, G, B = red, green, and blue coordinates
r, g, b = red, green, and blue chromaticity coordinates
S = saturation; Eq. (9)
T = model surface temperature, K
T_a = adiabatic wall temperature, K
T_i = model initial temperature, K
t = time, s
x^* = semi-infinite penetration depth, m
α = thermal diffusivity, $k/\rho c$, m^2s^{-1}
γ = $h\sqrt{(t/\rho ck)}$; Eq. (4)
λ = wavelength of reflection, m
ρ = substrate density, kgm^{-3}
ϕ = angle of illumination

Introduction

A CRITICAL feature of hypersonic vehicle design is the requirement to accommodate the thermal loads that the vehicle will experience during flight. To do this efficiently (i.e., without substantial overengineering), the aerodynamic heating mechanisms must be fully understood. Increasingly, modern computational fluid dynamics (CFD) tools are being used to predict the heating loads on complex shapes, but to do this with confidence, the CFD codes must themselves be validated by comparison with experimental data. These data must be of high fidelity and provide high spatial resolution in critical areas on the vehicle where the heating mechanisms may be complex. Often, the validation experiments need not involve the full vehicle geometry but may concentrate on specific types of flow that a simpler model might simulate.

A good example of this latter case concerns the measurement and prediction of heating loads in the complex interference flow region near a wing–body or fin–body junction: a reasonable simulation of the flowfield, with all of the major features present, can be created by using a fin-flat plate geometry.[1,2] Nevertheless, even with simple models, the demands on the instrumentation required to measure the details of complex heating distribution are quite considerable. Increasingly, techniques that are able to provide a high-resolution map of the surface temperature are being employed to measure the heating distribution on models that are experiencing complex flows. Such techniques include the use of thermographic paints and phosphors and infrared as well as liquid crystal thermography, the subject of this paper. Each technique has its advantages and disadvantages in terms of ease of use, cost, and quality of data obtained.

Temperature-sensitive and phase-change paints have been used successfully to estimate peak heating levels and transition on models in high-speed flows,[3,4] but the method is not well suited for obtaining a detailed map of the heating distribution in complex flow regions; in addition, the response of the coating to the thermal environment is not reversible, necessitating a fresh application of paint for each test. The use of thermographic phosphors is becoming more widespread in hypersonic testing,[5,6] as it overcomes many of the disadvantages just noted. In this technique, a thin layer of phosphor paint is applied to the wind-tunnel model, and when illuminated with ultraviolet light during a test, electrons in the paint surface become excited and emit visible light as they subsequently decay to lower energy

Graham T. Roberts is a lecturer in the Department of Aeronautics and Astronautics at the University of Southampton, having obtained his B.Sc. and Ph.D. degrees there in 1976 and 1985, respectively. His doctoral thesis concerned heat transfer in two-phase and chemically reacting flows. He returned to the University in 1986 after working in the aerospace industry as a Principal Engineer with Negretti Aviation, where he was concerned with gas turbine instrumentation. His main research interests include hypersonic aerothermodynamics and heat transfer, electric propulsion, and atomic oxygen effects on spacecraft. He has authored or coauthored over 30 technical papers and reports in these areas.

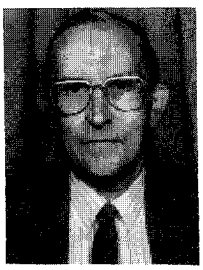

Robin A. East is Emeritus Professor of the University of Southampton. He was previously Professor of Aeronautics and Head of the Department of Aeronautics and Astronautics at the University of Southampton from 1985 to 1990. He has authored and coauthored over 90 papers and reports dealing with hypersonic aerodynamics, hypersonic facilities and instrumentation, heat transfer, and unsteady flows. He received his Ph.D. in aeronautical engineering from the University of Southampton in 1960 and has taught at that institution since 1963. He is an Associate Fellow of the AIAA and a Fellow of the Royal Aeronautical Society (RAeS) and Vice Chairman of the Aerodynamics Group Committee of the RAeS.

Received March 23, 1995; revision received May 28, 1996; accepted for publication June 6, 1996.

levels. The decay occurs at a rate that is temperature dependent, and hence the intensity of fluorescence provides an indication of the local surface temperature (the reader is advised to see Ref. 7 for further details of this technique). A recently reported development of a related technique offers the promise of simultaneous pressure and temperature mappings being obtained from a single application of a luminescent paint that is sensitive to the partial pressure of oxygen.[8]

In the past, infrared techniques have suffered from poor spatial resolution, but rapid advances in hardware technology are being made and data with high spatial resolution are now being obtained[9,10]; however, the equipment required is expensive to purchase, quantification of the data from the images obtained can be difficult because of the rather long image acquisition times, and special, infrared compatible optical access to the working section is required. Liquid crystal thermography is a heat-flux measurement technique that is also becoming more widely used, but mainly in low-speed, low heat-flux situations. With this technique, the liquid crystals (which, like the phosphors mentioned earlier, are also applied as a thin layer to the model) react to changing surface temperatures by changing color; providing a suitable calibration can be adopted, the color distribution can be interpreted in terms of heat flux. Although in principle the technique is cheap and simple to implement, in practice there are several problems and limitations that must be taken into account, especially when being used in short-duration, intermittent wind-tunnel facilities for measuring the (often high) surface heat fluxes experienced by models in hypersonic flows. These problems are discussed in this paper. However, while we recognize the technique's limitations, with careful experimental technique and data analysis, we will show that high-fidelity data can be obtained in this application using liquid crystals.

Properties of Thermochromic Liquid Crystals

Liquid crystals are substances that have a molecular structure intermediate between that of a crystalline solid and an isotropic liquid. As such, they possess the mechanical properties of liquids but the optical properties of crystalline solids; in particular, some liquid crystal substances, known as cholesteric (or chiral nematic) liquid crystals, are extremely optically active and react to changes in temperature and/or shear by changing color. This peculiar optical behavior is brought about by the molecular structure of these materials: the molecules are thin, rod-like structures that, in the nonisotropic liquid (i.e., crystalline) form, have their long axes aligned in a certain direction. In the so-called smectic phase the molecules form layers, each with their long axes pointing in the same direction; this phase is optically inactive. However, upon heating, the material may progress to what is known as a cholesteric or chiral nematic phase, where again the molecules are arranged in layers with the long axes aligned in a certain direction, but the direction progressively changes from one layer to the next to form a twisted, helical structure (Fig. 1). The chiral nematic phase is optically active. Upon further heating the liquid crystal may undergo a further phase transition to the isotropic liquid, which is again optically inactive. For further details the reader is advised to see Ref. 11 and manufacturers' handbooks, e.g., Ref. 12.

The ability to change color by changing the temperature and/or shearing the liquid crystals is a result of Bragg-like scattering of incident white light caused by the helical structure of the chiral nematic phase: in effect, the incident light is selectively reflected back from the liquid crystal layer according to the Bragg diffraction equation

$$\lambda = Pn\cos\phi \qquad (1)$$

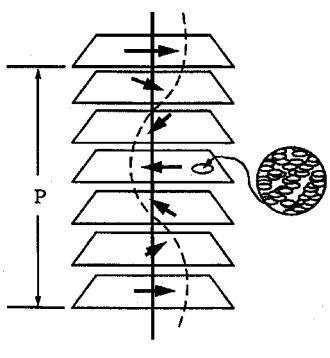

Fig. 1 Liquid crystal chiral nematic phase.

Note that, in the preceding, ϕ is the angle of the incident light beam measured from the normal to the surface. Equation (1) is a rather simplistic representation of the optical response, in that it predicts a single wavelength of reflection for given values of P, n, and ϕ. In practice, a range of wavelengths is reflected back, the bandwidth of which is governed by the local optical arrangement (angle of illumination and viewing angle, wavelength of illumination, etc.), the thickness of the liquid crystal layer, and the ambient conditions.[11] Nevertheless, under many circumstances a dominant wavelength of reflection (or color), which is broadly described by Eq. (1), can be identified under given conditions; it is evident that, for normal illumination, the dominant wavelength of reflection is of the same order of magnitude as the pitch of the liquid crystal helix. The latter can be tailored by the manufacturer so that, at any given temperature, the reflected wavelength can lie anywhere between the infrared and the ultraviolet. Clearly, for most convenient usage, the reflected wavelength should lie in the visible part of the spectrum. Changing the temperature or the action of shear alters the pitch of the helix and hence the reflected wavelength: in effect when illuminated with white light the liquid crystal layer changes color.

This type of optical activity has many uses, the most obvious being thermometry and, in particular in aerodynamic testing, the measurement of shear stress. The latter application was first investigated by Klein and Margozzi[13] and has subsequently been developed to a mature stage by many other workers,[14–18] including a recent application to the investigation of hypersonic boundary-layer transition.[19] Liquid crystal thermometry was first proposed as a means of measuring heat fluxes by Klein[20] and, again, has been developed to a mature stage by many others.[11,21–27] Several reviews of past work with thermochromic liquid crystals applied to low-speed flows have been published.[28–30] Their use in hypersonic flows was first reported in Ref. 31, and they have subsequently been employed successfully both as a nonquantitative surface flow visualization/diagnostic technique[32,33] and quantitatively to determine the surface heating rate.[1,2,34–41]

All optically active liquid crystals are sensitive to both temperature and shear, but the relative sensitivity can be adjusted by the manufacturer to suit a particular application. Temperature-sensitive (or thermochromic) liquid crystals are rendered insensitive to shear by microencapsulation: small droplets of the liquid crystals are contained in transparent spheres, typically of $\mathcal{O}(10)$-μm diameter, made from a suitable polymer. Microencapsulation has the added advantage of reducing the liquid crystals' sensitivity to contamination from solvents, etc. Heating the crystals causes the helical pitch to reduce, which, from Eq. (1), causes the reflected wavelength to shorten. Hence, upon heating, the liquid crystals will change from the optically inactive (colorless) smectic phase to the optically active cholesteric phase (labeled S-Ch in Fig. 2) through the visible spectrum from red to violet and then turn colorless again at high temperatures as the crystals undergo a second phase change from the cholesteric to isotropic liquid structure (labeled Ch-I in Fig. 2). The color play is generally reversible and exhibits negligible hysteresis in the steady state (the temporal response is discussed later), which, in practical terms, means that a single application of liquid crystals to a model can be used repeatedly (usually until the coating is ablated or otherwise damaged). However, if the isotropic phase transformation temperature is exceeded, the crystals can exhibit hysteresis:

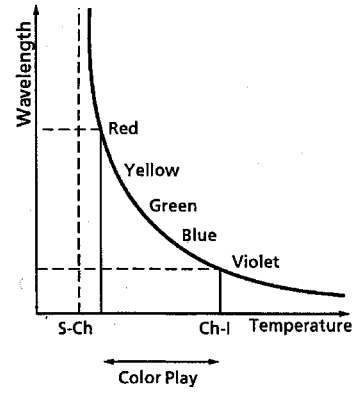

Fig. 2 Typical liquid crystal color response.

they may remain blue in color until they are cooled below the red-start (smectic-cholesteric phase-change) temperature, whereupon the hysteresis disappears and the color play becomes reversible again. Usually this phenomenon causes little practical difficulty.

The temperature range over which the liquid crystals reflect visible light is termed the color-play bandwidth and is usually characterized by the red-start and the blue-start temperatures; mixtures may be formulated by the manufacturer to suit the customer's red-start and bandwidth requirements. The red-start ranges currently offered by manufacturers lie between −30 and 115°C. Bandwidths may be narrow (1°C or less), in which case surface isotherms will be indicated, or wide $\mathcal{O}(10)$°C, in which case a full mapping of a model's surface temperature may be obtainable. Note that the color variation with temperature is nonlinear, with red usually occupying a rather small temperature range and blue quite a large range; hence, when subjected to a high heat flux (with attendant high-temperature gradient within the layer), a liquid crystal layer of finite thickness appears to be blue. This effect was investigated in Ref. 42, where it was shown that the response is monochromic for heat fluxes of $\mathcal{O}(10^4)$ Wm^{-2} but that, for larger heat fluxes, a broad band (blue) response occurs that must be allowed for, or otherwise overcome, to estimate the surface temperature correctly. This will be discussed further presently.

As described earlier, Eq. (1) suggests that the perceived color response is sensitive to angle of illumination; it is also sensitive to viewing angle.[25,42] In Ref. 42 (also reported in Ref. 11) it is shown that the peak reflection wavelength reduces by about 30 nm when the viewing angle is varied from the normal to about 60 deg to the normal (note that this wavelength variation will depend on both the particular liquid crystal formulation being used and the local surface temperature); although this does not seem to be a large variation, the change in perceived color could be interpreted as a significant change in surface temperature.

On highly curved models this effect must be accounted for in the analysis of results. In principle, if the liquid crystal response to lighting and viewing angle is known (e.g., by precalibration), it should be possible to apply a color correction to the data providing the lighting/viewing angles can be estimated over the entire model surface; alternatively, a color vs temperature calibration could be carried out on the curved surfaces of the model in situ in the tunnel and the calibration subsequently applied to the data.[40] Neither are straightforward, but, fortunately, the sensitivity is not large providing the lighting/viewing angles are less than 20–30 deg from the normal. In Ref. 25 it is shown that the sensitivity to viewing angle is reduced if the illumination and viewing of the model is carried out on a common axis; when coupled with an independent color calibration system, the on-axis lighting/viewing configuration allows the perceived surface temperature variation to be reduced to ±0.25°C (compared with ±0.6°C off-axis) for angles up to ±25 deg from the normal. However, in many instances it may not be possible to carry out the illumination and viewing on-axis (e.g., as a result of equipment limitations and/or reflected glare from wind-tunnel test-section windows), in which case some increase in measurement uncertainty must be tolerated.

Another problem of particular importance in using thermochromic liquid crystals in short-duration wind-tunnel facilities is that the response of the liquid crystal layer is not instantaneous. Besides the time taken to elevate the liquid crystals to their color-play temperature range (which is dependent on the initial model temperature and the magnitude of the applied heat flux), the crystals take a finite time to respond mechanically (by adjusting the pitch of the helix) to the changing thermal environment. This latter time has been determined experimentally to be on the order of a few milliseconds[43,44] and is related to the viscosity of the liquid crystal formulation[15]; it must be allowed for in any heat-flux estimation. This lag also imposes a limitation on the applicability of the liquid crystal technique: it cannot be used in situations where the applied heat-flux is changing rapidly, nor can it be used in very short run duration facilities. In Ref. 44, although some response was observed from a liquid crystal layer applied to a model experiencing large heat fluxes [$\mathcal{O}(10^5)$ Wm^{-2}] in a shock tube with a run time of approximately 1–3 ms, it was evident that this was not an equilibrium response and for practical purposes the liquid crystal technique was of little use under these conditions; however, liquid crystals have been used successfully both qualitatively[33] and semiquantitatively (e.g., see Refs. 36 and 37) in gun tunnels where the run duration is of the order 20–40 ms.

Practical Aspects

Both steady-state[21,27,30] and transient[1,24,26,34–41] techniques can be employed to measure heat fluxes using thermochromic liquid crystals; however, only the latter is suited to tests using short-duration wind-tunnel facilities, as the model does not usually have time to attain an equilibrium temperature. With the transient technique the observed color change during testing is used as an indication of the changing surface temperature. By using an appropriate theoretical model of the thermal response of the wind-tunnel model to the (suddenly applied) heat flux, the latter can be deduced from the temperature changes. In this respect, the technique is similar to those more conventionally employed in short-duration facilities (e.g., thin-film resistance or surface thermocouple gauges[45]), except, of course, the coverage and spatial resolution of the thermographic technique is much superior; however, as mentioned earlier, the temporal response is inferior and, for various reasons that will be discussed, the uncertainty in the heat flux estimation is generally slightly greater than that obtained using more conventional sensors.

Model Design and Preparation

The choice of model material is largely dictated by the magnitude and duration of the thermal pulse it is expected to experience. Models experiencing modest heat fluxes $\mathcal{O}(10^4)$ Wm^{-2} for durations $\mathcal{O}(1)$ s are best fabricated from an insulating (plastic) material to ensure a reasonable temperature rise, whereas models experiencing higher heat fluxes and/or longer flow durations may better be fabricated from a suitable metal to limit the temperature rise, although in this case lateral conduction effects may not be negligible. In any case, it is important that the model has a matt black surface finish as this provides a nonreflective background against which the liquid crystal colors will appear most brilliant.

Suitable black plastic materials are available (e.g., perspex, polyethersulfone, etc.); ideally, these should have thermal properties {in particular the thermal product $[\sqrt{(\rho ck)}]$} similar to that of the liquid crystal material [typical values are $\rho = 1020$ kgm^{-3}, $c = 1800$ $Jkg^{-1}K^{-1}$, $k = 0.2$ Wm^{-2}, and thermal product $\sqrt{(\rho ck)} = 600$ $Jm^{-2}K^{-1}s^{-1/2}$ (Ref. 11)], so that the two materials appear to be homogeneous as far as heat conduction is concerned. When metal models are used, a coating of black paint is required; in this case the analysis of the thermal response is more complicated since the liquid crystals and black paint have thermal properties very different from that of the underlying metal.

This latter situation was considered in Ref. 35, in which the response of a multilayered substrate to a suddenly applied, constant heat flux was modeled numerically; the results indicate that the surface temperature rise is initially rapid, being dominated by the properties of the (insulating) layers of liquid crystals and black paint but that, after the switch-point (the time taken for the thermal pulse to penetrate these layers), it is dominated by the underlying metallic surface and is therefore much slower. In principle, even with the multilayered substrate, it is possible to derive the heat flux from the observed temperature rise at any (known) time after run commencement.

The liquid crystals are usually applied to the model using an artist's airbrush. Reference 25 describes good practice for this. Experience has shown that the optimum thickness of liquid crystal layer for color reflection lies in the region of 30–50 μm when wet, corresponding to a dry thickness of about 10–20 μm (i.e., about one or two capsule diameters). Note that even microencapsulated liquid crystals are sensitive to chemical contamination (especially from organic solvents) and to ultraviolet radiation; hence it is best to store a model in a clean, dark environment when not in use.

Image Acquisition

A variety of techniques exist for image acquisition and storage: data can be recorded photographically, as an analog signal on a

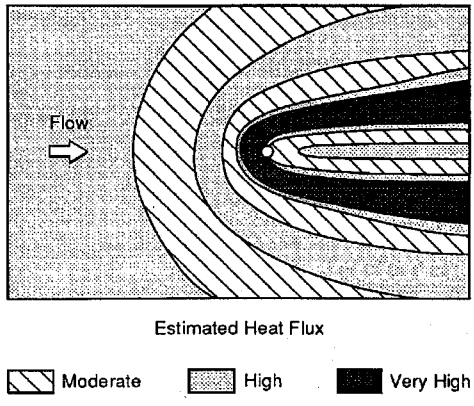

Fig. 3 Qualitative heat-flux estimation from a single photographic image.[32]

videotape or digitally on a computer disk. The first is cheap to implement and can produce high-quality images. Qualitative judgements of areas of high/low heat flux are easily made from such images [e.g., Fig. 3—redrawn from Ref. 32—shows the zones of high/low heat flux near a normal, sonic jet issuing from a flat plate into a hypersonic (Mach 6.7) freestream flow], but quantification of the data from such images is difficult, not least because the color rendition of the image is very much dependent on the film processing and color determination is usually subjective.

For example, in Ref. 34 the heat fluxes on test models were estimated by comparing (by eye) the colors obtained from a single photographic image (taken at a predetermined time after run start) with those obtained from a static liquid crystal color/temperature calibration. Besides introducing considerable uncertainty, the subjective interpretation of such images resulted in the estimation of heat fluxes lying within broad bands, which in effect degraded the spatial resolution of the data. The technique can be improved slightly by comparing the colors displayed on a test model with those on a calibration model (e.g., a flat plate) experiencing a known and similar range of heat fluxes.[35] By ensuring that the initial temperatures of the test and calibration models are the same and that the images are obtained at the same time after the start of the run, the heat flux may be estimated on the test model. However, in Ref. 35 the color comparison remained subjective and so the spatial resolution and overall accuracy of the technique were only marginally enhanced.

Both the accuracy and the spatial resolution of the heat-flux estimation can be improved by analyzing data obtained from several images (providing these are obtained at known times after the start of the flow). In the authors' experience attempts at obtaining multiple photographic images at high framing rates (using a high-speed camera) have largely been unsuccessful as the image quality is severely degraded, which makes the subjective interpretation of the color display even more difficult. However, the subjectivity can be removed by digital analysis. For this, the images are best recorded on videotape or directly onto the framestore of a computer. A charge-coupled device (CCD) camera (rather than a conventional raster-type video camera) is required for this, since full-frame images are then acquired practically instantaneously. The framing rate is determined either by that of the video recorder or by that of the frame grabber. There are color video recorders available with framing rates in excess of 400 images per second, but, in practice, more modest rates are often acceptable with wind-tunnel facilities with run times $\mathcal{O}(1)$ s. The majority of the authors' liquid crystal work has been performed in the Southampton University Light Piston, Isentropic Compression (LPIC) hypersonic wind-tunnel facility (which has a run time of approximately 0.5 s) using a video system with a framing rate of 50 images per second. Once recorded on videotape, the images may be replayed and digitized by a frame grabber and the data recorded on disk.

For improved image quality, it is best to bypass the video recorder and store the images directly onto the buffer memory of the frame grabber; however, in cases where the memory is limited (e.g., a limit of two full-resolution color frames is typical of many systems), the framing rate will be reduced and dictated by the speed with which the data can be transferred to the host computer memory. Therefore there is a tradeoff to be made between image quality and quantity.

The color response of the liquid crystals (and, to some extent, the image acquisition system employed) will be highly dependent on the type of illumination used. In most systems it is best to use an illumination system that approximates closely to a white light source; many video systems with CCD cameras offer a white-balance facility, where a correction is applied to equalize the signals from the red, green, and blue guns when viewing a reference white (or gray) card, thereby counteracting the effects of nonwhite illumination. Most experiments are carried out with background (ambient) light excluded, although in Ref. 25 a technique is described that can reduce the sensitivity of the overall system to background lighting. Occasionally it may be advantageous to use a light source with a narrow bandwidth, particularly if certain colors (corresponding to particular isotherms on the model) are to be identified. For example, in Ref. 44 a helium-neon laser was used to illuminate the model and the reflected light from the model passed through a narrow bandwidth filter to identify a particular isotherm; however, note that, in these experiments, the reflected light intensity was very low and required the use of a photomultiplier detector.

It should be obvious that whatever light source is employed should be of insufficient power to heat the model significantly before or during the wind-tunnel run. The intensity of illumination should be as uniform as possible across the model, although often this is not achievable either because of limited optical access to the working section or because of stray reflections from adjacent surfaces or from the model itself.

To counteract such reflections, it may be possible to use another optical property of cholesteric liquid crystals: they are circularly dichroic, which means that unpolarized light is resolved into its two circularly polarized components (left hand and right hand), one of which is transmitted through the liquid crystal unaffected, and the other is reflected. This optical behavior is also a consequence of the helical structure of the liquid crystal.[12] If the transmitted light is then reflected off a solid surface, the polarization will change sense (i.e., right hand will become left hand, and vice versa), while the component reflected by the liquid crystal layer retains its original sense. Most thermochromic liquid crystal formulations reflect left-handed polarized light; hence, if the incident illumination is passed through a left-hand polarizing filter, all of the (polarized) light incident on the liquid crystal layer should be reflected. If the reflected light is also viewed through a left-hand polarizing filter, all stray light of the opposite circular polarization (including any that has been transmitted through the liquid crystal layer and reflected off the underlying model surface) will be attenuated; in this manner the effects of stray reflections (e.g., from test-section windows) and glare on the model can be reduced and the overall image contrast and quality should be improved. However, in the authors' experience it has been found that, depending on the quality of the filters employed, some of the selectively reflected light may also be attenuated and/or color shifted, and so the use of such filters must be treated with caution.

Image Analysis and Heat-Flux Estimation

In the following discussion it will be assumed that, with a facility run duration of $\mathcal{O}(1)$ s, liquid crystal images of a test model have been recorded and digitized as described earlier. It is further assumed that all of the conditions concerning lighting/viewing angle have been satisfied by optimizing the configuration of the apparatus as described in the preceding sections.

Heat-Flux Estimation

With the transient technique, the temperature rise on the test model (deduced from the observed color change of the liquid crystals as described later) is used to estimate the heat flux to the model; to do so, a suitable thermal model of the unsteady heat conduction process must be formulated. Such a model is easily obtained providing the following criteria are satisfied: 1) the heat flux is applied suddenly and remains constant throughout the run, 2) the thermal properties of the model [in particular the thermal product $\sqrt{(\rho ck)}$] are homogeneous, and 3) the heat conduction process is one-dimensional and the model is effectively semi-infinite in extent.[45]

In many intermittent wind-tunnel facilities the flow starting process is relatively rapid and so the criterion that the heat flux is applied suddenly is satisfied. In those facilities (e.g., blowdown tunnels) where this is not the case, the model must be shielded from the flow while the tunnel starting process is under way. Techniques for achieving this involve either initially mounting the model outside the flow and rapidly inserting it into the flow once it has become correctly established in the working section or by allowing the flow to establish around the model while it is protected by a thermally insulating shroud, which is then suddenly removed (e.g., by explosive detonation).

The convective heat flux to the model is given by

$$q_w(t) = h[T_a - T(t)] \tag{2}$$

For the heat flux to remain constant, the flow properties must remain invariant throughout the run and the temperature difference $[T_a - T(t)]$ must not change appreciably. Although the former is commonly satisfied, in facilities where the run duration is lengthy, the heat fluxes are high, and the model is manufactured from an insulating material (e.g., plastic), the latter criterion may not be. For example, in the Southampton University LPIC facility, the adiabatic wall temperature is approximately 600 K and the surface temperature on a plastic model may typically rise from 290 K to in excess of 350 K during the 0.5-s run time, leading to a 20% reduction in heat flux. Fortunately, although the heat flux is changing throughout this period, the constant flow properties ensure that the heat transfer coefficient does remain constant (it is assumed that the temperature rise is insufficient to alter the state of the boundary layer). The heat transfer coefficient may be estimated from[45]

$$\frac{T(t) - T_i}{T_a - T_i} = 1 - erfc(\gamma)\exp(\gamma^2) \tag{3}$$

where

$$\gamma = h\sqrt{t/\rho ck} \tag{4}$$

and $erfc(\gamma)$ is the complementary error function for γ.

By evaluating the model temperature at time t, the left-hand side of Eq. (3) is known and yields a unique value of γ from which, using Eq. (4) and the known properties of the model substrate, h may be evaluated. The heat flux may then be evaluated from Eq. (2) if desired, although it is often more convenient to use h to define a nondimensional heat transfer coefficient (Stanton or Nusselt number).

Equation (3) is only valid if the preceding criteria 1 and 2, are also satisfied. Homogeneous thermal behavior is ensured by matching the thermal product $\sqrt{(\rho ck)}$ of the model substrate with that of the liquid crystals. In practice matching may not be exactly achieved, but in Ref. 39 it was shown that, for a typical thickness of liquid crystal layer (10–20 μm), the error introduced if the mismatch in thermal product is $\pm 30\%$ is less than $\pm 10\%$ for $t \geq 20$ ms and continues to diminish rapidly with further increase in time. The model must continue to behave as though it is semi-infinite in extent throughout the measuring period (i.e., the conductive heat pulse must not reflect off the back wall of the model). The thickness required for semi-infinite behavior is[45]

$$x^* = 4\sqrt{\alpha t} \tag{5}$$

For typical plastic materials, this depth is approximately 1 mm for $t = 1$ s; for metals it is $\mathcal{O}(10)$ mm. The preceding can also be used as a guide to estimate the influence of lateral conduction on the spatial resolution of the data obtained, although the formula given in Eq. (5) is rather pessimistic in this case.[40]

In situations where any of the preceding criteria are not satisfied, the thermal model becomes much more complex. Generally, such situations require some form of numerical analysis to extract the heat flux for a measured surface temperature rise (e.g., see Ref. 35).

Surface Temperature Estimation

Color information from digitized images is usually stored as separate red, green, and blue (R, G, and B) components. Color (and hence temperature) determination directly from these components is, however, difficult since the values also contain information

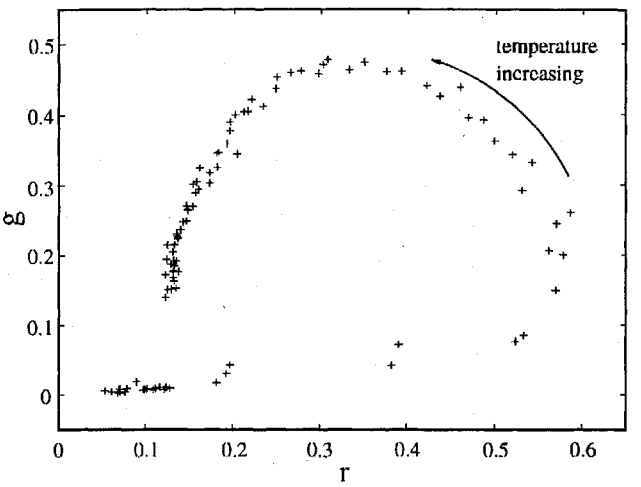

Fig. 4 Variation of g and r with temperature.

concerning the light intensity, which may not be as uniform as desired. One method of reducing the effect of the latter is to use the chromaticity coordinates r, g, and b, where

$$r = \frac{R}{R+G+B}, \qquad g = \frac{G}{R+G+B}$$
$$b = \frac{B}{R+G+B} \tag{6}$$

In principle, it is possible to calibrate the temperature response of a particular set of liquid crystals to the variation in r, g, and b under given lighting conditions (e.g., see Fig. 4, noting that $r+g+b=1$). However, the reverse process (i.e., deducing the surface temperature from a measured set of r, g, and b values) is not so straightforward, as there are three independent variables (e.g., r, g, and T).

A method commonly employed to overcome this is to transform the R, G, and B coordinates into hue, saturation, and intensity (H, S, and I), where

$$H = 90 - \tan^{-1}(F_1/\sqrt{3}) + F_2 \tag{7}$$

and

$$F_1 = \frac{2R - G - B}{G - B} \tag{8}$$

and $F_2 = 0$ for $G \geq B$ and 180 for $G < B$,

$$S = 1 - \frac{\min(R, G, B)}{I} \tag{9}$$

$$I = \frac{R+G+B}{3} \tag{10}$$

In this coordinate system, the color information is contained solely in the value of H; the definition provided by Eq. (7) is slightly different from that usually quoted elsewhere (e.g., Ref. 22) in that the results are given in degrees, illustrating that the hue is an angular representation of color, with the primary colors R, G, and B taking hue values of 0, 120, and 240 deg, respectively (note that R can also take on the value of 360 deg).

For a given optical arrangement, it is possible to determine the variation of hue exhibited by the liquid crystals with temperature by performing a suitable static calibration experiment, from which a single curve (which is independent of lighting intensity[23]) should result. Figure 5a shows such a calibration obtained from a relatively low red-start temperature, small bandwidth batch of crystals (Merck type TCS552). Below 25°C the crystals remain colorless, and because the model is black, the hue value should be indeterminate (ideally R, G, and B all equal to zero, but because of unwanted reflections and system offsets, this is not usually the case). Above 25°C, the liquid crystals exhibit a visible optical activity and the hue value increases, transitions through the 0/360 deg red hue value at approximately 26°C, and then continues to increase monotonically

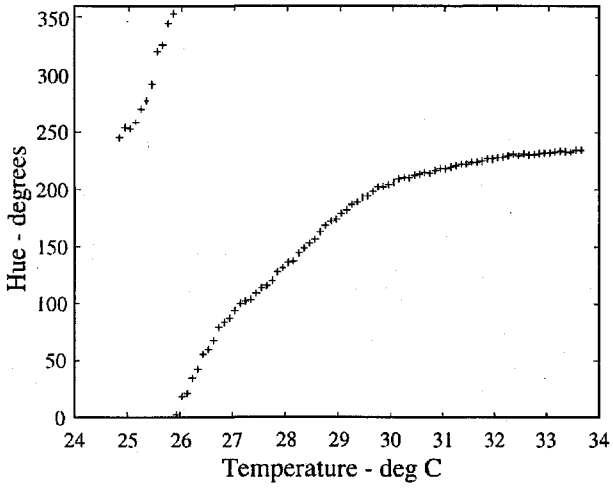

a) Unmodified

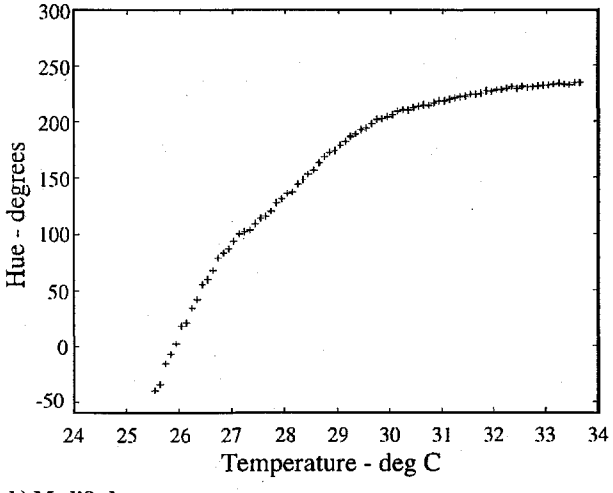

b) Modified

Fig. 5 Variation of hue with temperature.

with further increase in temperature until the liquid crystals turn deep violet/colorless at approximately 34°C.

Because of the circular nature of the hue representation of color, the discontinuity in the curve shown in Fig. 5a can be removed by subtracting 360 deg from all hue values above that corresponding to the colorless liquid crystal ($H \sim 250$ deg); the resulting curve is shown in Fig. 5b. Providing the response of the model and liquid crystal layer to the applied heat flux in the wind-tunnel experiment approximates to that of the static calibration experiment, the curve shown in Fig. 5b can be used to determine the surface temperature [and hence heat-flux or heat transfer coefficient via Eqs. (2–4)] on the model. To do so, a polynomial curvefit of temperature vs hue is applied to the calibration data, from which the surface temperature can be deduced for a given (measured) value of hue. In practice, the curve is only applied within a certain band of temperatures because the sensitivity of the crystals at high temperatures (as the isotropic liquid phase transition is approached) decreases to such an extent that random fluctuations in hue values (e.g., as a result of the prescence of noise on the images) produces unrealistically large fluctuations in temperature.

The preceding technique has been applied to the jet interaction problem originally studied in Ref. 32; the preliminary results are reported in Ref. 41, and some of them are reproduced here. Figure 6 shows a schematic of the model geometry, which comprised a flat plate with a single, circular, sonic jet of 3-mm diameter approximately 140 mm downstream of the leading edge. The freestream Mach number was ~6.7, the test gas was nitrogen, and the flow over the flat plate was laminar. Figure 7 shows the variation in the undisturbed (i.e., flat plate, no jet) heat transfer coefficient (h_u) with distance from the leading edge, estimated from the measured hue

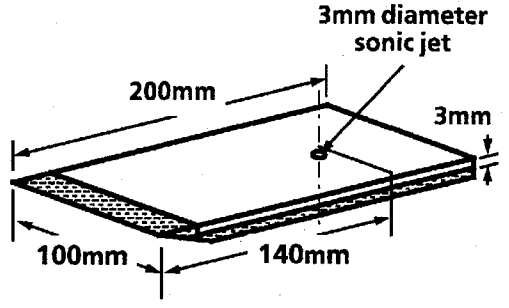

Fig. 6 Schematic of flat plate model with transverse jet.

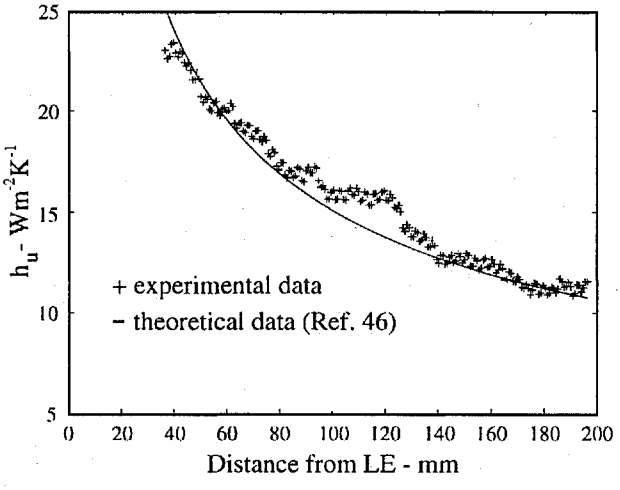

Fig. 7 Variation of heat transfer coefficient with distance for flat plate (no jet).

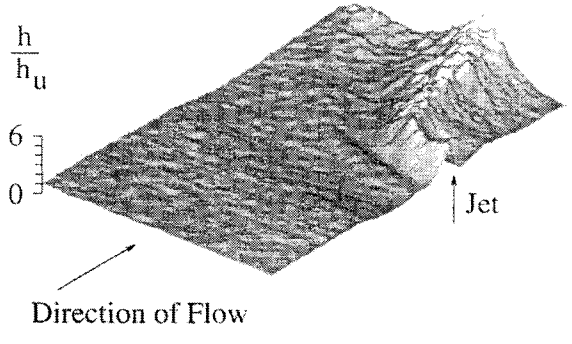

Fig. 8 Isometric map of normalized heat transfer coefficient for flat plate flow with jet.

values using a static calibration curve similar to that illustrated in Fig. 5b. Also shown in Fig. 7 are the results obtained using the semi-empirical correlation of Ref. 46 for a laminar flat plate flow under the given experimental conditions. Although there is some noise on the experimental data, the overall level of agreement is good (generally within ±10% of the empirical correlation) and indicates the confidence with which the technique may be applied to such flows. The magnitude of the heat flux in these experiments was $\mathcal{O}(10^4)$ Wm^{-2}.

Figure 8 is an isometric map of the heat transfer coefficient (normalized with respect to the undisturbed, flat plate value) obtained with the jet flow switched on (the jet plenum pressure was 1.0 bar and the jet gas argon). For clarity, only half the flowfield is shown (exploiting the symmetry in the flowfield) and the jet location on the centerline of the plate is indicated. The region illustrated extends about 100 mm upstream of the jet, 60 mm downstream, and 50 mm laterally. In this instance the pixel resolution was slightly less than 1 mm^2. Evidently the interaction of the jet with the oncoming hypersonic flow has created a flowfield with a complex heating distribution on the plate. In general, the magnitude of the heat transfer has been enhanced ($h/h_u > 1$) by the interaction, although in some regions (identified by complementary surface oil-flow investigations[32] as regions of separated and recirculating flow) the heat transfer has

been reduced ($h/h_u < 1$). This image should be compared with the qualitative plot shown in Fig. 3: it is obvious that the same heating patterns are present. The ability of the liquid crystal thermographic technique to identify and—more importantly—to quantify these complex variations in surface heating is clearly demonstrated.

Unfortunately, the preceding method can only be applied when a static calibration of hue vs temperature is valid. As described earlier, this is unlikely for situations where the heat flux is large (as a result of the distorting effect of the temperature gradient within the liquid crystal layer). To overcome this limitation, a dynamic calibration technique may be employed in which the color response of the crystals under test conditions is compared with simultaneous measurements of temperature from surface-mounted thermocouples.[40] Alternatively, the technique employed in Ref. 35 (where the colors obtained from test and calibration models subjected to similar ranges of heat fluxes are compared) could be performed using digital image analysis techniques, thereby removing any subjectivity in interpretation.

In Ref. 39 a variant of the narrow bandwidth technique was employed in which the heat transfer coefficient was deduced by noting the location of the red-start contour on a series of video images. In effect this contour corresponds to a known isotherm and hence a particular value of γ [Eq. (3)]. By noting the time at which the contour was observed at a particular location, the heat transfer coefficient may be evaluated using Eq. (4). The rationale behind applying this technique to high heat flux situations is that, no matter how large the heat flux, the surface will always register a red color first. Again, the results of this method were compared with the semi-empirical theory of Ref. 46 for a flat plate with a turbulent boundary layer, in which the magnitude of the heat flux was $\mathcal{O}(10^5)$ Wm^{-2}, and good agreement was noted.

The method was applied successfully to flat plate/fin configurations, tested at a freestream Mach number of 6.2, also with a turbulent upstream boundary layer. The results[1] were presented as a series of contours of nondimensional heat transfer coefficients, where the normalizing factor is the undisturbed (i.e., no fin) heat transfer coefficient at the fin leading-edge location. The contours obtained for a blunt, unswept fin with a leading-edge diameter $D = 10$ mm have been reproduced in Fig. 9a and are to be compared with the same contours resulting from numerical simulations[2] of the flowfield, shown in Fig. 9b. Although the agreement between the experimental results and numerical simulations is not perfect (in particular the upstream influence of the fin interaction is greater in the numerical simulation than measured experimentally), both show similar features: evidently a complex heating distribution is created by the interaction of the fin bow shock with the boundary layer on the flat plate, causing the oncoming flow to separate ahead of the fin and then to roll up into a series of horseshoe vortices.

In this respect the flowfield is similar to that of the jet interaction problem described earlier except that, in this turbulent boundary-layer flowfield, the interference effects created by the fin have caused the local heating only to increase, even at the point of separation (indicated approximately by the outermost contours in Figs. 9a and 9b). Experimentally, a fivefold enhancement in heating near the fin base was observed (indicated by the innnermost contour), although it is known that the heating levels nearer the fin base are very much greater than this (the numerical simulations predict a 25-fold enhancement). In this instance (and with this technique generally) both the spatial resolution and the ability to resolve the rapidly changing surface temperatures caused by the high heat fluxes present are strongly influenced by the framing rate of the video system employed: a high framing rate is clearly desirable for optimum resolution.

Accuracy of Results

The preceding discussion has shown how high spatial resolution data can be obtained using liquid crystal thermography. Figure 5 shows that, in the temperature range where the crystal response is most sensitive, the surface temperature may be resolved to an estimated uncertainty of ± 0.1°C over the majority of the color-play bandwidth. This value will vary according to the bandwidth of the particular batch of liquid crystals in use: a narrow bandwidth batch will offer high sensitivity, but be more prone to temperature gradient

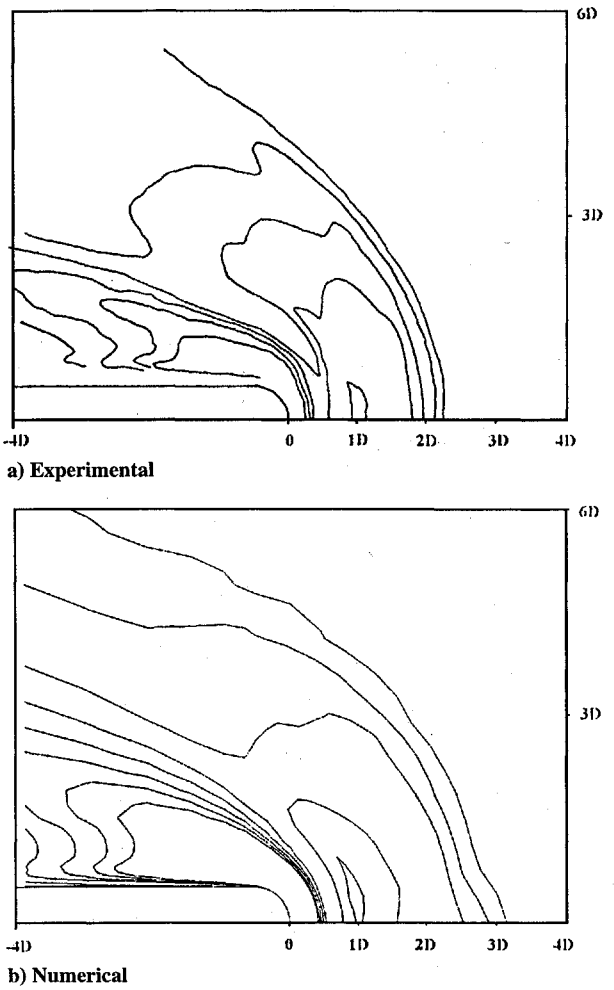

Fig. 9 Contours of normalized heat transfer coefficients for flat plate with fin.

effects, which will weaken and distort its color response. Note, however, that the accurate determination of the temperature differences $[T(t) - T_i]$ and $[T_a - T_i]$ are required to reduce the uncertainty in the heat-flux determination. This places equally stringent requirements on the determination of T_a and, in particular, T_i. Taking all of these factors into account, the overall uncertainty in heat-flux determination is estimated to be typically in the region of $\pm 10\%$.[40] Although this figure is somewhat greater than the $\pm 5\%$ typical uncertainty in heat-flux estimation using more conventional transient techniques (thin-film or thermocouple gauges), it is considered that the benefits of ease and economy of instrumentation, coupled with the ability to provide high spatial resolution data, often outweigh the reduced accuracy, especially when complex flows are to be investigated.

Conclusions

The basic principles underlying the use of thermochromic liquid crystals for heat flux determination in short run duration [$\mathcal{O}(1)$ s] hypersonic facilities have been outlined. Procedures for model construction, liquid crystal calibration, and image acquisition and analysis have also been described. It has been shown that, despite the inherent limitations of the technique, high spatial resolution data with accceptable uncertainty bounds can be obtained. Consequently, the technique is an invaluable tool for aiding the understanding and complementing numerical studies of complex flows.

Acknowledgments

The authors would like to acknowledge the help of R. P. Clarke, P. H. Schuricht, and Z. Wu (Beijing Institute of Aerodynamics) in the preparation of this paper. Hallcrest Liquid Crystal Technology Ltd. is thanked for giving permission for Figs. 1 and 2 to be reproduced from its catalog, as are all authors of papers kindly donated for this review.

References

[1]Haq, Z., Roberts, G. T., and East, R. A., "Interference Heating Near Fin/Body Junctions on Hypersonic Vehicles," *Proceedings of the 1st European Symposium on Aerothermodynamics for Space Vehicles*, European Space Agency, SP-318, Noordvijk, The Netherlands, 1991, pp. 171–176.

[2]Tutty, O. R., Roberts, G. T., and East, R. A., "Numerical Study of Fin/Body Interference Heating Effects at Hypersonic Speeds," *Proceedings of the 2nd European Symposium on Aerothermodynamics for Space Vehicles*, European Space Agency, SP-367, Noordvijk, The Netherlands, 1995, pp. 51–56.

[3]Keyes, J. W. "Shock Interference Peak Heating Measurements Using Phase Change Coatings," *Journal of Spacecraft and Rockets*, Vol. 13, No. 1, 1976, pp. 61–63.

[4]Cattafesta, L. N., Iyer, V., Masad, J. A., King, R. A., and Dagenhart, J. R., "Three-Dimensional Boundary-Layer Transition on a Swept Wing at Mach 3.5," *AIAA Journal*, Vol. 33, No. 11, 1995, pp. 2032–2037.

[5]Micol, J. R., "Aerothermodynamic Measurement and Prediction for Modified Orbiter at Mach 6 and 10," *Journal of Spacecraft and Rockets*, Vol. 32, No. 5, 1995, pp. 737–748.

[6]Buck, G. M., "Surface Temperature/Heat Transfer Measurement Using Two-Color Thermographic Phosphors," AIAA Paper 91-0064, Jan. 1991.

[7]Merski, N. R., "A Relative-Intensity Two-Color Phosphor Thermographic System," NASA TM 104123, May 1991.

[8]Buck, G. M., "Simultaneous Luminescence Pressure and Temperature Measurement System for Hypersonic Wind Tunnels," *Journal of Spacecraft and Rockets*, Vol. 32, No. 5, 1995, pp. 791–794.

[9]Carlomagno, G. M., "Characterisation of Hypersonic Flow in a Wind Tunnel," *Proceedings of the IUTAM Symposium on Aerothermochemistry of Spacecraft and Associated Hypersonic Flows*, Univ. of Provence, Marseille, France, 1992, pp. 437–442.

[10]Henckels, A., Kreins, A. F., and Maurer, F., "Applications of Infrared Measurement to Hypersonic Facilities," *Proceedings of the 18th International Symposium on Shock Waves*, Vol. 1, Springer–Verlag, Berlin, 1992, pp. 651–656.

[11]Jones, T. V., "The Use of Liquid Crystals in Aerodynamic and Heat Transfer Testing," *Proceedings of the 4th International Symposium on Transport Phenomena in Heat and Mass Transfer*, Elsevier, Amsterdam, The Netherlands, 1992, pp. 1242–1273.

[12]Parsley, M., "The HALLCREST Handbook of Thermochromic Liquid Crystal Technology," Hallcrest Products Inc., Glenview, IL, 1991.

[13]Klein, E. J., and Margozzi, A. P., "Exploratory Investigation on the Measurement of Skin Friction by Means of Liquid Crystals," *Israel Journal of Technology*, Vol. 7, Nos. 1–2, 1969, pp. 173–180.

[14]Ciliberti, D. F., Dixon, G. D., and Scala, L. C., "Shear Effects on Cholesteric Liquid Crystals," *Molecular Crystals and Liquid Crystals*, Vol. 20, No. 1, 1973, pp. 27–36.

[15]Bonnett, P., Jones, T. V., and McDonnell, D. G., "Shear Stress Measurement in Aerodynamic Testing Using Cholesteric Liquid Crystals," *Liquid Crystals*, Vol. 6, No. 3, 1989, pp. 271–280.

[16]Toy, N., Savory, E., Hoang, Q. H., and Gaudet, L., "Calibration and Use of Shear Sensitive Liquid Crystals in Aerodynamic Testing," *Proceedings of the 15th International Congress on Instrumentation in Aerospace Simulation Facilities*, Inst. of Electrical and Electronics Engineers, New York, 1993, pp. 49.1–49.6.

[17]Reda, D. C., Muratore, J. J., and Heineck, J. T., "Time and Flow-Direction Responses of Shear-Stress-Sensitive Liquid Crystal Coatings," *AIAA Journal*, Vol. 32, No. 4, 1994, pp. 693–700.

[18]Reda, D. C., and Muratore, J. J., "Measurement of Surface Shear Stress Vectors Using Liquid Crystal Coatings," *AIAA Journal*, Vol. 32, No. 8, 1994, pp. 1576–1582.

[19]Aeschliman, D. P., Croll, R. H., and Kuntz, D. W., "Shear-Stress-Sensitive Liquid Crystals for Hypersonic Boundary-Layer Transition Detection," *Journal of Spacecraft and Rockets*, Vol. 32, No. 5, 1995, pp. 749–757.

[20]Klein, E. J., "Application of Liquid Crystals to Boundary Layer Flow Visualisation," AIAA Paper 68-376, Jan. 1968.

[21]Simonich, J. C., and Moffat, R. J., "Liquid Crystal Visualisation of Surface Heat Transfer on a Concavely Curved Turbulent Boundary Layer," *Journal of Engineering for Gas Turbines and Power*, Vol. 106, No. 3, 1984, pp. 619–627.

[22]Toy, N., and Savory, E., "Quantitative Assessment of Surface Temperatures Using Liquid Crystals and Digital Imaging," *Proceedings of the IMechE Conference on Optical Methods and Data Processing in Heat and Fluid Flow*, Inst. of Mechanical Engineers, London, 1992, pp. 141–144.

[23]Camci, C., Kim, K., and Hippensteele, S. A., "A New Hue Capturing Technique for Quantitative Interpretation of Liquid Crystal Images Used in Convective Heat Transfer Studies," *Journal of Turbomachinery*, Vol. 114, No. 4, 1992, pp. 765–775.

[24]von Wolfersdorf, J., Hoecker, R., and Sattelmayer, T., "A Hybrid Transient Step-Heating Heat Transfer Measurement Technique Using Heater Folis and Liquid-Crystal Thermography," *Journal of Heat Transfer*, Vol. 115, No. 2, 1993, pp. 319–324.

[25]Farina, D. J., Hacker, J. M., Moffat, R., and Eaton, J., "Illuminant Invariant Calibration of Thermochromic Liquid Crystals," *Journal of Experimental Thermal and Fluid Sciences*, Vol. 9, No. 1, 1994, pp. 1–12.

[26]Wang, Z., Ireland, P. T., and Jones, T. V., "An Advanced Method of Processing Liquid Crystal Video Signals from Transient Heat Transfer Experiments," *Journal of Turbomachinery*, Vol. 117, No. 1, 1995, pp. 184–189.

[27]Stasiek, J., Collins, M. W., Ciofalo, M., and Chew, P. E., "Investigation of Flow and Heat Transfer in Corrugated Passages—1. Experimental Results," *International Journal of Heat and Mass Transfer*, Vol. 39, No. 1, 1996, pp. 149–164.

[28]Kasagi, N., Moffat, R. J., and Hirata, M., "Liquid Crystals," *Handbook of Flow Visualisation*, Hemisphere, Washington, DC, 1989, pp. 105–124.

[29]Moffat, R. J., "Experimental Heat Transfer," *Proceedings of the 9th International Heat Transfer Conference*, Hemisphere, Washington, DC, 1990, pp. 187–205.

[30]Baughn, J. W., "Liquid Crystal Methods for Studying Turbulent Heat Transfer," *International Journal of Heat and Fluid Flow*, Vol. 16, No. 5, 1995, pp. 365–375.

[31]Schöler, H., "Application of Encapsulated Liquid Crystals on Heat Transfer Measurements in the Fin/Body Interaction Region at Hypersonic Speed," AIAA Paper 78-777, April 1978.

[32]Powrie, H., Ball, G. J., and East, R. A., "Comparison of the Interactions of Two and Three Dimensional Transverse Jets with a Hypersonic Free Stream," *Proceedings of the AGARD Conference on Computational and Experimental Assessment of Jets in Cross Flow*, AGARD CP-534, 1993, pp. 20.1–20.7.

[33]Zanchetta, M. A., and Hillier, R., "Laminar-Turbulent Transition at Hypersonic Speeds: The Effects of Nose Blunting," *Proceedings of the 2nd European Symposium on Aerothermodynamics for Space Vehicles*, European Space Agency, SP-367, Noordvijk, The Netherlands, 1995, pp. 207–212.

[34]Haq, Z., Roberts, G. T., and East, R. A., "Interference Heating in Corner Regions at Hypersonic Speeds," *Proceedings of the International Conference on Hypersonic Aerodynamics*, Royal Aeronautical Society, London, 1989, pp. 27.1–27.14.

[35]Smith, A. J. D., and Baxter, D. R. J., "Liquid Crystal Thermography for Aerodynamic Heating Measurements in Short Duration Hypersonic Facilities," *Proceedings of the 13th International Congress on Instrumentation in Aerospace Simulation Facilities*, Inst. of Electrical and Electronics Engineers, New York, 1989, pp. 104–112.

[36]East, R. A., "Applications of Liquid Crystal Thermography to Hypersonic Flow," *Proceedings of the 18th International Symposium on Shock Waves*, Vol. 1, Springer–Verlag, Berlin, 1992, pp. 643–650.

[37]Babinsky, H., and Edwards, J. A., "Quantitative Heat Transfer Measurement Using Liquid Crystal Thermography in an Hypersonic Gun Tunnel," *Proceedings of the IUTAM Symposium on Aerothermochemistry of Spacecraft and Associated Hypersonic Flows*, Univ. of Provence, Marseille, France, 1992, pp. 419–424.

[38]Babinsky, H., and Edwards, J. A., "The Application and Analysis of Liquid Crystal Thermographs in Short Duration Hypersonic Flow," AIAA Paper 93-0182, Jan. 1993.

[39]Haq, Z., "Hypersonic Vehicle Interference Heating," Ph.D. Thesis, Univ. of Southampton, Dept. of Aeronautics and Astronautics, Southampton, England, UK, 1993.

[40]Babinsky, H., "A Study of Roughness in Hypersonic Turbulent Boundary Layers," Ph.D. Thesis, College of Aeronautics, Cranfield Univ., Bedford, England, UK, 1994.

[41]Mudford, N. R., Roberts, G. T., Schuricht, P. H., Ball, G. J., and East, R. A., "Interference Heating Effects Caused by a 3-D Transverse Jet in Hypersonic Flow," *Shock Waves, Proceedings of the 20th International Symposium on Shock Waves*, Vol. 1, World Scientific Publishing Co., Singapore, 1996, pp. 173–178.

[42]Bonnett, P., "Applications of Liquid Crystals in Aerodynamic Testing," Ph.D. Thesis, Dept. of Engineering Science, Univ. of Oxford, England, UK, 1989.

[43]Ireland, P. T., and Jones, T. V., "The Response Time of a Thermochromic Liquid Crystal Surface Thermometer," *Journal of Physics E: Scientific Instruments*, Vol. 20, No. 10, 1987, pp. 1195–1199.

[44]Zhang, Z. C., Roberts, G. T., and Pratt, N. H., "An Experimental Evaluation of Thermochromic Liquid Crystals for Surface Temperature and Heat-Flux Measurements in Shock Tube Flows," *Current Topics in Shock Waves, Proceedings of the 17th International Symposium on Shock Waves and Shock Tubes*, American Inst. of Physics CP-208, New York, 1990, pp. 618–623.

[45]Schultz, D. L., and Jones, T. V., "Heat Transfer Measurements in Short-Duration Hypersonic Facilities," AGARD-AG-165, Feb. 1973.

[46]Eckert, E. R. G., "Engineering Relations for Skin Friction and Heat Transfer to Surfaces in High Velocity Flows," *Journal of the Aerospace Sciences*, Vol. 22, Aug. 1955, pp. 585–587.

K. J. Weilmuenster
Associate Editor